Revised Version

SINP/TNP/2009/14

arXiv:0903.0202[hep-ph]

arXiv:0903.0202v2 [hep-ph] 28 Jul 2009

# Di-jet production at the LHC through unparticles

**Neelima Agarwal**[a 1], **M. C. Kumar**[b,c 2], **Prakash Mathews**[b 3], **V. Ravindran**[d 4], **Anurag Tripathi**[d 5]

*a) Department of Physics, University of Allahabad, Allahabad 211002, India.*

*b) Saha Institute of Nuclear Physics, 1/AF Bidhan Nagar, Kolkata 700 064, India.*

*c) School of Physics, University of Hyderabad, Hyderabad 500 046, India.*

*d) Regional Centre for Accelerator-based Particle Physics,*

*Harish-Chandra Research Institute, Chhatnag Road, Jhunsi, Allahabad 211 019, India.*

**Abstract**

We report the phenomenological impact of unparticles in the production of di-jet at the LHC. We compute the scalar, spin-1 and spin-2 unparticle contributions to the dijet cross sections and present our results in different kinematical distributions. We find that the scalar unparticle contribution is dominant over that of the spin-1 and spin-2 unparticles for the same coupling values.

[1]neel1dph@gmail.com
[2]mc.kumar@saha.ac.in
[3]prakash.mathews@saha.ac.in
[4]ravindra@hri.res.in
[5]anurag@hri.res.in

The Large Hadron Collider (LHC), will explore the origin of the spontaneous symmetry breaking which is responsible for giving masses to gauge bosons in the Standard Model (SM). Its main effort will be on the discovery of the elusive Higgs boson which is a signature of the spontaneous symmetry breaking and is the last missing particle of the SM. Even if Higgs Boson is discovered, many questions remain unanswered in the SM. This indicates to the existence of some New Physics (NP) at high energies beyond the SM. As the LHC will operate at high energies never attained before in any experiment, signals of NP beyond the SM could be discovered here. There are many possible NP scenarios, such as, supersymmetry, extra-dimensions etc. There are other interesting possibilities as well that have been thought of, especially involving scale or conformal symmetries. "Conformal collider physics" was recently discussed in [1]. Similarly the newly envisaged unparticle model [2], though does not address the problems of the SM, is interesting in its own right. This model is based on the curious possibility of scale invariant degrees of freedom coupling to the SM fields at low energies. In this model, at very high energies the SM couples weakly to a hidden sector, called Banks-Zaks (BZ) sector [3], via exchange of heavy particles of mass M. Effective theory below M contains interaction terms of the form

$$\frac{1}{M^k}\mathcal{O}_{SM}\mathcal{O}_{BZ}\,, \tag{1}$$

where $\mathcal{O}_{SM}$ and $\mathcal{O}_{BZ}$ are operators constructed out of SM and BZ fields respectively. This hidden sector is proposed to have a nontrivial infrared fixed point. One can take an effective field theory approach and integrate out high energy degrees of freedom. As the modes are integrated out the renormalization group flow takes us close to the IR fixed point. Near the fixed point, scale invariance emerges in the hidden sector below a scale $\Lambda_u$. The above interaction term below $\Lambda_u$ matches to

$$\frac{{\Lambda_u}^{d_{BZ}-d_u}}{M^k}\mathcal{O}_{SM}\mathcal{O}_u. \tag{2}$$

The operators $\mathcal{O}_u$ are scale invariant and scale with momenta with some scaling dimension $d_u$, which depends on the operator. $d_{BZ}$ is the mass dimension of $\mathcal{O}_{BZ}$ operator. Apart from an overall normalization, the scale invariance fixes the two-point function

of unparticle operators without requiring any detailed knowledge of the theory at high energies. Unparticle operators can have different tensor structures, such as scalar, vector or tensor. Here, in this study, we will consider scalar, spin-1 and spin-2 unparticles. The effective interaction for scalar and spin-1 unparticle consistent with the SM gauge symmetries are:

$$\mathcal{L}_{int} \supset \frac{\lambda_{s_1}}{4\Lambda_u^{d_s}} F^a_{\mu\nu}F^{a\mu\nu}\ \mathcal{O}_u + \frac{\lambda_{s_2}}{\Lambda_u^{d_s-1}}\ \bar{\psi}\psi\ \mathcal{O}_u\,, \tag{3}$$

$$\mathcal{L}_{int} \supset \frac{\lambda_v}{\Lambda_u^{d_v-1}}\ \bar{\psi}\gamma_\mu\psi\ \mathcal{O}^\mu_u\,, \tag{4}$$

where $\lambda_i$ are the dimensionless coupling constants of the scalar ($i = s_{1,2}$) and vector ($i = v$) unparticles, $d_i$ are the scaling dimension of scalar ($i = s$) and vector ($i = v$) unparticle operators.

For the spin-2 unparticle, we assume that the SM fields couple to unparticle operator $O_u^{\mu\nu}$ via the SM energy momentum tensor $T_{\mu\nu}$ :

$$\mathcal{L}_{int} \supset \frac{\lambda_t}{\Lambda_u^{d_t}} T_{\mu\nu}\ O_u^{\mu\nu}\,, \tag{5}$$

Tensor operator $O_u^{\mu\nu}$ which is traceless and symmetric has a scaling dimension $d_t$. Unitarity imposes constraint $d_s > 1$ on the scaling dimension of scalar unparticle [5] and scale invariance restricts $d_v, d_t \geq 3$ [6]. Scalar, tensor and vector unparticle propagators are given respectively by [6–8]

$$\int d^4x\ e^{-ik\cdot x}\langle 0|TO_u(x)O_u(0)|0\rangle = -i\ C_S \frac{\Gamma(2-d_s)}{4^{d_s-1}\Gamma(d_s)}(-k^2)^{d_s-2} \tag{6}$$

$$\begin{aligned}\int d^4x\ e^{-ik\cdot x}\langle 0|TO_u^{\mu\nu}(x)O_u^{\alpha\beta}(0)|0\rangle &= -i\ C_T \frac{\Gamma(2-d_t)}{4^{d_t-1}\Gamma(d_t+2)}(-k^2)^{d_t-2} \\ &\quad \times [d_t(d_t-1)(g_{\mu\alpha}g_{\nu\beta}+\mu\leftrightarrow\nu)+\ldots]\,,\end{aligned} \tag{7}$$

$$\begin{aligned}\int d^4x\ e^{-ik\cdot x}\langle 0|TO_u^{\mu}(x)O_u^{\nu}(0)|0\rangle &= +i\ C_V \frac{(d_v-1)\Gamma(2-d_v)}{4^{d_v-1}\Gamma(d_v+1)}(-k^2)^{d_v-2} \\ &\quad \times \left[g^{\mu\nu} - \frac{2(d_v-1)}{d_v-1}\frac{k^\mu k^\nu}{k^2}\right]\,,\end{aligned} \tag{8}$$

where $C_S, C_T, C_V$ are overall normalisation constants. The terms given by ellipses in Eq. (7) and the terms proportional to $k^\mu k^\nu$ in Eq. (8), do not contribute to di-jet production.

Recently unparticle phenomenology, in the context of present and future colliders has been explored in great detail [9]. At the LHC, in the case of unparticles, the study of di-jet was considered in [10] by considering only the $gg \to gg$ sub process assuming that the gluon flux would help this channel to dominate over the others. This analysis of [10] was prior to the results of [6], which in the context of unparticles pointed out the lower bounds on operator dimensions and dictates the tensor structure of the unparticle propagators. In our analysis we have taken note of the above points and consider all the sub processes that would contribute to the di-jet via the exchange of spin-0, spin-1 and spin-2 unparticles. Including all the subprocess is important as the gluon and quark operators couple to the scalar unparticle operators with different powers of the unparticle scale $\Lambda_u$ (see Eq. (3-5)). Hence the enhancement due to gluon flux at the LHC could be suppressed by the addition power of $\Lambda_u$ in the gluonic coupling to scalar unparticles.

The LHC can provide a testing ground for physics of unparticles if $\Lambda_u$ is of the order of a TeV. There are various important channels available at the LHC to explore the new physics at TeV scales, namely production of di-leptons, isolated photon pairs, di-jets etc. The importance of di-lepton and di-photon production channels in the context of unparticles were already studied in detail in [11] and [12, 13] respectively. In this article we will study the effects of scalar and spin-2 unparticles on the di-jet production rates at the LHC if the scale $\Lambda_u$ is of the order of a TeV. Di-jet production is an important discovery mode and many studies in the context of various new physics scenarios have been carried out, namely, SUSY searches [14], searches of the low mass strings [15]. Di-jet production has been used to probe spin-2 Kaluza-Klein gravitons appearing in the extra dimensional models [16–18].

To lowest order in strong coupling constant, di-jets arise from $2 \to 2$ scattering of partons. In the unparticle model the dijets could be produced due to the exchange of unparticles between SM particles. The partons in the final state hadronize to give two jets in the detectors. Signals of NP can be discovered because of the deviations they produce over the SM contributions. The unparticles can contribute through intermediate states

as well as via real emission. The former one can interfere with the SM contributions, while the later can lead to missing energy in the final state. In this article we will restrict ourselves to the effects coming from spin-0, spin-1 and spin-2 intermediate states. The parton level $2 \to 2$ subprocesses in the SM and in the unparticle scenario are

$$\begin{array}{lll} qq\prime \to qq\prime & qq \to qq & q\overline{q} \to q\overline{q} \\ q\overline{q} \to q\prime\overline{q}\prime & q\overline{q} \to gg & gg \to q\overline{q} \\ qg \to qg & gg \to gg & \end{array}$$

Here we have used primes to distinguish quark flavours. For the scalar case, not all of the above processes contribute. The first term in Eq. (3) describes the coupling of gauge fields to scalar unparticles giving $gg \to gg$ process. The second term couples fermions to scalar unparticles, which allows subprocesses that have only fermions in the initial and the final states. We shall study the effects of these two terms in Eq. (3) separately. In the case of vector unparticles, there are no processes involving gluons (Eq. (4)) that would contribute to the dijet process.

The leading order SM matrix elements are of order $g_s^2$, where $g_s$ is the strong coupling constant and those in the unparticle model are of order $\kappa^2$, where $\kappa = \lambda_t/\Lambda_u^{d_t}, \quad \lambda_{s_1}/\Lambda_u^{d_s}$, $\lambda_{s_2}/\Lambda_u^{d_s-1}, \lambda_v/\Lambda_u^{d_v-1}$. The matrix element square takes the following form:

$$g_s^4 \left|\mathcal{M}_{SM}\right|^2 \;+\; \kappa^4 \left|\mathcal{M}_u\right|^2 \;+\; g_s^2\kappa^2(\mathcal{M}_{SM}\mathcal{M}_u^* + \mathcal{M}_{SM}^*\mathcal{M}_u)$$

where the interference of the SM with the unparticle mediated processes will be sensitive to phase coming from $(-k^2)^d$ in the propagators given in Eq. (6-8). In the table (1), we list the matrix elements square, summed (averaged) over final (initial) state colors and spins, for SU(N) gauge theory with fermions in the fundamental representation. The SM ones agree with those existing in the literature [19]. We have not listed the subprocesses such as $\overline{q}\ \overline{q} \to \overline{q}\ \overline{q}$, $\overline{q}\ \overline{q}\prime \to \overline{q}\ \overline{q}\prime$ and $\overline{q}g \to \overline{q}g$ as they can be obtained from the rest using charge conjugation. In addition, there are processes that are related by crossing symmetry *viz.* $\overline{q}\ q\prime \to \overline{q}\ q\prime$ is obtained from $q\ q\prime \to q\ q\prime$.

The matrix elements for pure unparticle contribution and interference with SM for spin-0 coupling through the first term in (3) are given below (see Eq. (10)). Here, only $gg \to gg$ subprocess contributes. The factor $(-k^2)^{d-2}$ in propagators is complex for a $s$-channel propagator and is real for $u$- and $t$-channel propagators.

$$|\mathcal{M}_u|^2 \overset{gg\to gg}{=} \frac{1}{16(N^2-1)} \Big(\mathcal{D}_u Re(\mathcal{D}_s)\ s^2\ u^2 + \mathcal{D}_t Re(\mathcal{D}_s)\ s^2\ t^2 + \mathcal{D}_t\mathcal{D}_u\ t^2\ u^2\Big) + \frac{1}{16}\left(\mathcal{D}_u^2\ u^4 + \mathcal{D}_t^2\ t^4 + |\mathcal{D}_s|^2\ s^4\right) \tag{9}$$

$$2\mathcal{R}e\Big(\mathcal{M}_{SM}\mathcal{M}_u^*\Big) \overset{gg\to gg}{=} -\frac{N}{2(N^2-1)}\left(Re(\mathcal{D}_s)\ \frac{s^4}{ut} + \mathcal{D}_u\ \frac{u^4}{st} + \mathcal{D}_t\ \frac{t^4}{us}\right) \tag{10}$$

where

$$\mathcal{D}_s = -C_S \frac{\Gamma(2-d_s)}{4^{d_s-1}\Gamma(d_s)}(-s)^{d_s-2}. \tag{11}$$

Table (2) contains the corresponding matrix element square for spin-0 unparticle interacting via the second term in Eq. (3). In table (4), we give the matrix element square for spin-2 unparticles with $\mathcal{D}_s$ as defined by

$$\mathcal{D}_s = -C_T \frac{\Gamma(2-d_t)}{4^{d_t-1}\Gamma(d_t+2)}(-s)^{d_t-2} d_t(d_t-1). \tag{12}$$

The matrix elements for spin-1 are given in table (3) with corresponding $\mathcal{D}_s$ defined by

$$\mathcal{D}_s = +C_V \frac{(d_v-1)\Gamma(2-d_v)}{4^{d_v-1}\Gamma(d_v+1)}(-s)^{d_v-2} \tag{13}$$

The $t$ ($u$)-channel propagators can be obtained by the replacement $s \to t(u)$.

We now study invariant mass $Q$ distribution, namely $d\sigma/dQ$, of the di-jet for the LHC with a center of mass of energy $\sqrt{S} = 14$ TeV. We have implemented all the parton level matrix element squares in a Monte Carlo based code that can accommodate all the experimental cuts relevant for the phenomenological study. A 1/2 factor for sub processes involving identical particles in the final state has been taken care of, when the angular integration is done over the range $-1 \le \cos(\theta) \le 1$. We use the leading order (LO) CTEQ 6L parton distribution functions (PDF) with the corresponding value of LO strong coupling constant $\alpha_s(M_Z) = 0.118$ and 5 light quark flavours. The factorization

scale $\mu_F$ that appears in the PDFs and the renormalization scale $\mu_R$ in $\alpha_s(\mu_R^2)$ are identified with a single scale $Q$. In accordance with the CMS [20], we restrict the jets to satisfy rapidity cut $|\eta| < 1$ and the transverse momentum cut $p_T > 50$ GeV for each final state jet. We choose the scale $\Lambda_u$ to be 2 TeV below which the scale invariance in the BZ sector sets in. The dimensionless coupling constants are chosen to be $\lambda_t, \lambda_{s1}, \lambda_{s2}, \lambda_v = 0.9$ (see Eq. (3-5)) for all our phenomenology and we fix $C_T, C_S, C_V = 1$ appearing in the normalization of the propagators given in Eq. (6-8). Notice that the di-jet production at the LHC has a huge SM back ground unlike Drell-Yan or the di-photon production case. We will also study the sensitivity of our results to the scaling dimensions of the unparticle operators.

In the left panel of Fig. 1, we have plotted various subprocess contributions to the di-jet invariant mass distribution for spin-0 case (Eq. (3)) as a function of $Q$ between 600 GeV and 1800 GeV. Interference of unparticle contribution with SM is added to those coming from pure unparticles in plotting these curves. Solid line gives the prediction in the SM. We note that $gg \to gg$ contribution resulting from the first term of Eq. (3) is numerically small compared to those coming from the second term. All the quark (and anti-quark) initiated subprocesses contribute almost equally for most of the $Q$ range. In the right panel, we have shown the sensitivity of the scaling dimension $d_s$ to $d\sigma/dQ$ distribution as a function of $Q$. Various curves here correspond to different values of $d_s$ in the range 1.0-2.0. It is clear from the right panel that the unparticle effects in the fermion initiated processes can be visible above $Q = 800$ GeV for scaling dimension closer to 1.99. As we deviate from $d_s = 1.99$ to lower values, the effects get washed away completely for a wide range of $Q$.

In Fig. 2 we have plotted the invariant mass distribution resulting from the spin-2 unparticles (see Eq. (5)). Scale invariance restricts the scaling dimension to be greater than 3. In the left panel we have used $d_t = 3.001$ for giving various subprocess contributions. In the right panel of fig (2) we show the i variation of the signal with varying $d_t$ over a wide range 3.0-4.0. We find that the spin-2 unparticles do not give signifi-

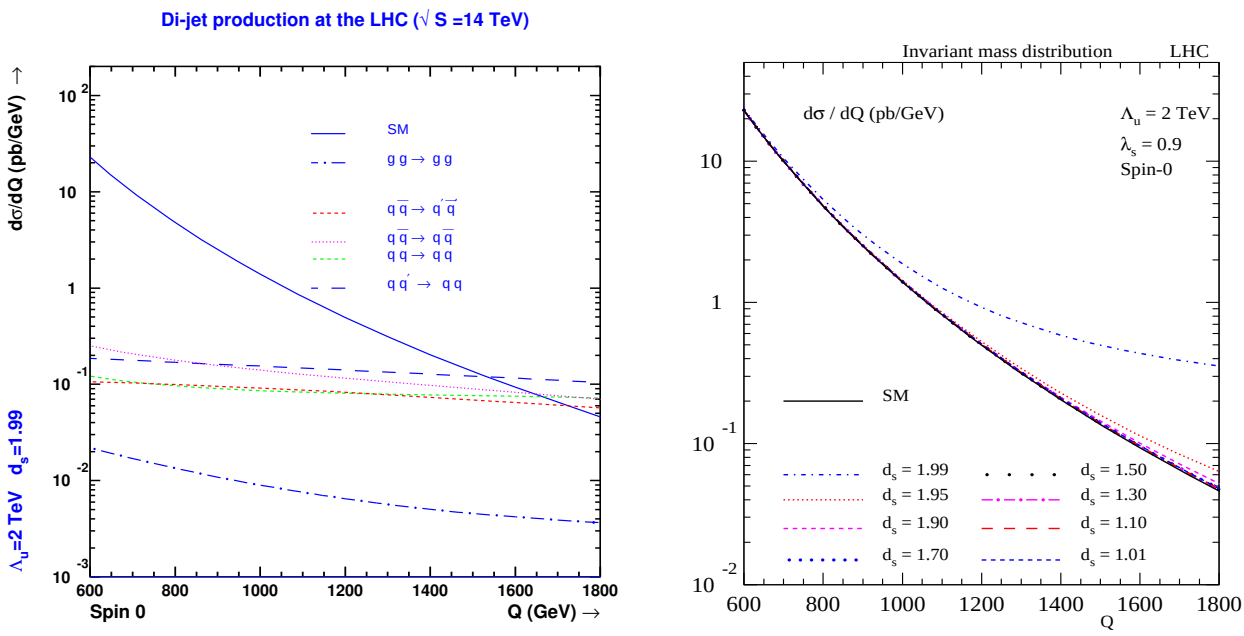


Figure 1: $d\sigma/dQ$ for di-jet production with spin-0 unparticles. The couplings are taken to be $\lambda_{s1,s2} = 0.9$ Left panel: Subprocess contribution. Right panel: Variation with scaling dimension.

cant enhancement over the SM di-jet cross-section. The tensor unparticle contribution is smaller than that of the scalar unparticle due to the additional $\Lambda_u$ suppression (see Eq. (5)) and large $d_t$ value. This is in contrast to the di-photon production, for example, which gets significant enhancements from spin-2 unparticles as well.

In Fig. 3, we present the scalar unparticle contribution in the transverse momentum distributions of the jets. Because of the rapidity cut $|\eta| < 1$ on the jets, the events will be transverse in nature. In the limit where the momentum of the jet is in the transverse direction, it is easy to see that $p_T = Q/2$, where $Q$ is the invariant mass of the di-jet. As $Q$ is required to be less than $\Lambda_u$ in the unparticle sector, we choose $Q^{max} = 0.9\ \Lambda_u$ which translates into $p_T^{max} = Q^{max}/2$. As $p_T$ is directly related to $Q$, the unparticle contribution is expected to be visible in the high $p_T$ region as can be seen from the figure (left panel). The steep fall in the distribution close to 900 GeV is due to the limit on $p_T$ ($< p_T^{max}$).

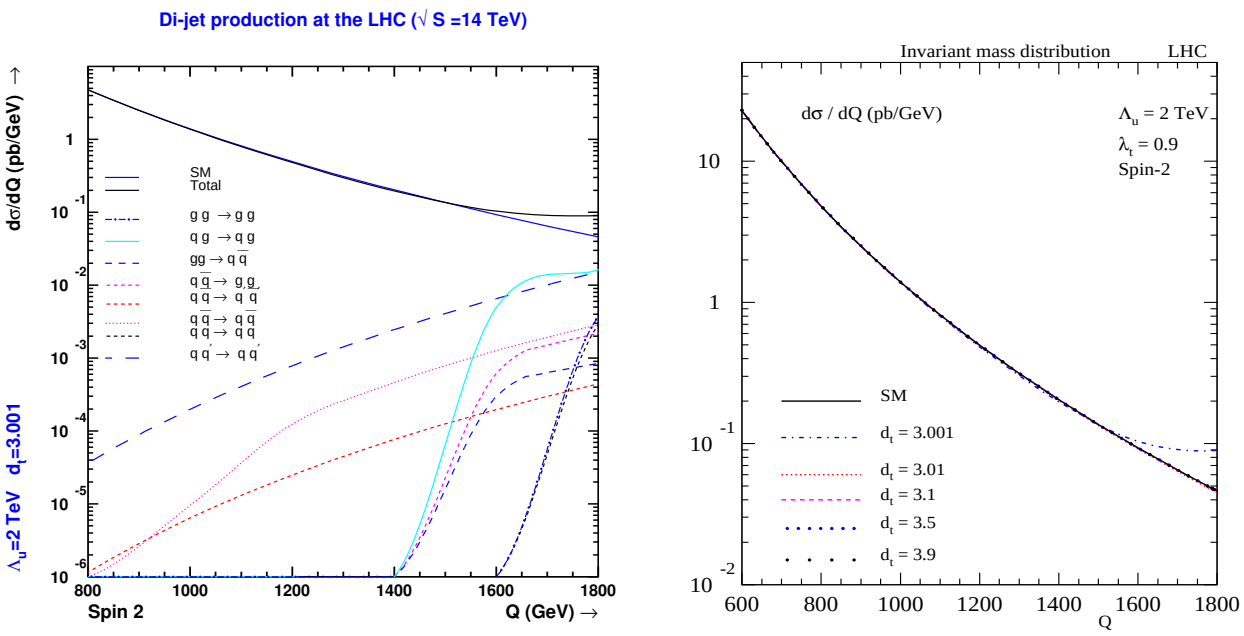


Figure 2: Spin-2 subprocess contributions to the di-jet invariant mass distribution for $\Lambda_u$=2TeV and $d_t = 3.001$.

In Fig. 4 we present rapidity distributions for scalar unparticles. In evaluating this distribution for non-identical final state partons, we have added to the matrix element square $|M(t,u)|^2$ the $t \leftrightarrow u$ piece $|M(u,t)|^2$ as experimentally it is difficult to distinguish between different partonic jets. We have integrated over $Q$ in the region $1200 < Q < Q^{max}$ where the unparticle contribution is dominant over the SM background and present the rapidity distribution in the range $0 < \eta < 0.8$ (Fig. 4).

Finally we present the results for spin-1 unparticles. In Fig. 5 we present invariant mass and $p_T$ distributions for spin-1 unparticles. In the left panel we show the variation of invariant mass distribution with the scaling dimension $d_v$ and in the right panel for $d_v = 3.001$ we have plotted the $p_T$ distributions. In Fig. 6 the rapidity distribution is plotted in the range $0 < \eta < 0.8$ for $d_v = 3.001$. We note that the signal is not significantly different from SM unless we are very close to $d_v = 3$.

To summarise, in this article, we have studied the effects of scalar, spin-1 and spin-2 unparticles to the di-jet production at the LHC. We have considered two SM scalar op-

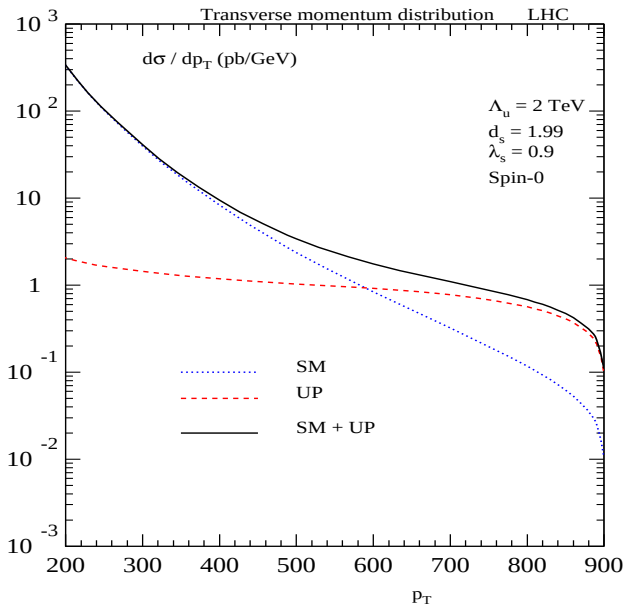


Figure 3: Scalar unparticle contribution to transverse momentum distributions of the jet in the di-jet production for $\Lambda_u = 2$ TeV for $d_s = 1.99$.

erators constructed out of quark (anti-quark) and gluon field operators that couple to the scalar unparticles. The SM operator which couples to the vector unparticle operator is constructed out of the quark (anti-quark) fields. The spin-2 tensor unparticles couple to a second rank SM operator which we take it to be SM energy-momentum tensor. We have computed all the parton level cross sections and implemented in a Monte Carlo code that can easily incorporate all the experimental cuts. We have presented various subprocess contributions coming from scalar and tensor unparticles along with the SM contributions. This includes the interference of unparticle effects with the SM. We find that the scalar unparticle effects are larger compared to those of spin-1 and spin-2 unparticles. Moreover, for a wide range of $Q$ and scaling dimensions, the di-jet cross section is insensitive to spin-1 and spin-2 unparticles. However, the scalar unparticles can give significant enhancements in the invariant mass, rapidity and $p_T$ distributions over the SM predictions.

**Acknowledgments:** The work of NA and MCK is supported by CSIR Senior Research

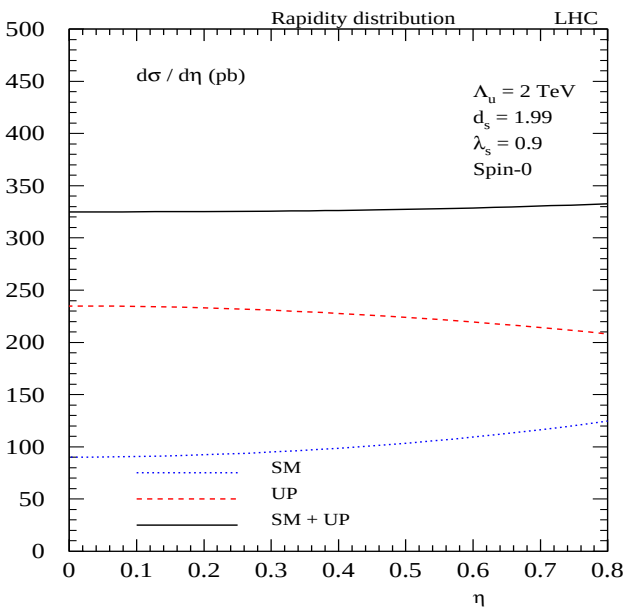
Rapidity distribution
LHC
dσ / dη (pb)
Λu = 2 TeV
ds = 1.99
λs = 0.9
Spin-0
SM
UP
SM + UP
500
450
400
350
300
250
200
150
100
50
0
0
0.1
0.2
0.3
0.4
0.5
0.6
0.7
0.8
η

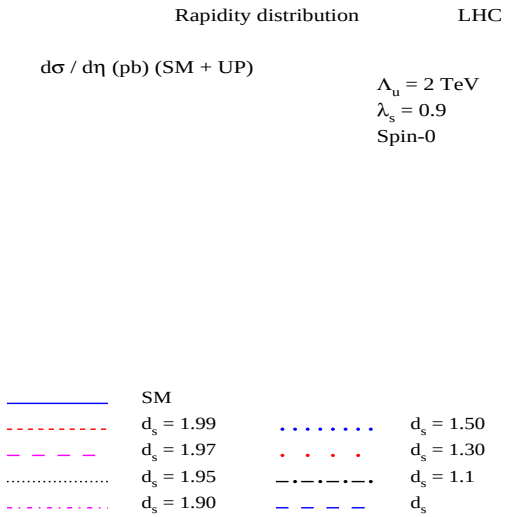
Rapidity distribution
LHC
dσ / dη (pb) (SM + UP)
Λu = 2 TeV
λs = 0.9
Spin-0
SM
ds = 1.99
ds = 1.97
ds = 1.95
ds = 1.90
ds = 1.50
ds = 1.30
ds = 1.1
ds

[6] B. Grinstein, K. A. Intriligator and I. Z. Rothstein, Phys. Lett. B **662** (2008) 367 [arXiv:0801.1140 [hep-ph]].

[7] H. Georgi, Phys. Lett. B **650** (2007) 275 [arXiv:0704.2457 [hep-ph]].

[8] K. Cheung, W. Y. Keung and T. C. Yuan, Phys. Rev. Lett. **99** (2007) 051803 [arXiv:0704.2588 [hep-ph]].

[9] K. Cheung, W. Y. Keung and T. C. Yuan, AIP Conf. Proc. **1078** (2009) 156 [arXiv:0809.0995 [hep-ph]]. A. Rajaraman, AIP Conf. Proc. **1078**, 63 (2009) [arXiv:0809.5092 [hep-ph]], and references therein.

[10] A. T. Alan, arXiv:0711.3272 [hep-ph].

[11] P. Mathews and V. Ravindran, Phys. Lett. B **657** (2007) 198 [arXiv:0705.4599 [hep-ph]].

[12] M. C. Kumar, P. Mathews, V. Ravindran and A. Tripathi, Phys. Rev. D **77** (2008) 055013 [arXiv:0709.2478 [hep-ph]].

[13] M. C. Kumar, P. Mathews, V. Ravindran and A. Tripathi, arXiv:0804.4054 [hep-ph].

[14] L. Randall and D. Tucker-Smith, Phys. Rev. Lett. **101** (2008) 221803 [arXiv:0806.1049 [hep-ph]].

[15] L. A. Anchordoqui, H. Goldberg, D. Lust, S. Nawata, S. Stieberger and T. R. Taylor, Phys. Rev. Lett. **101** (2008) 241803 [arXiv:0808.0497 [hep-ph]].

[16] P. Mathews, S. Raychaudhuri and K. Sridhar, JHEP **0007**, 008 (2000) [arXiv:hep-ph/9904232].

[17] D. Atwood, S. Bar-Shalom and A. Soni, Phys. Rev. D **62** (2000) 056008 [arXiv:hep-ph/9911231].

[18] D. K. Ghosh, P. Mathews, P. Poulose and K. Sridhar, JHEP **9911** (1999) 004 [arXiv:hep-ph/9909567].

[19] B. L. Combridge, J. Kripfganz and J. Ranft, Phys. Lett. B **70** (1977) 234.

[20] A. Bhatti *et al.*, J. Phys. G **36** (2009) 015004 [arXiv:0807.4961 [hep-ex]].

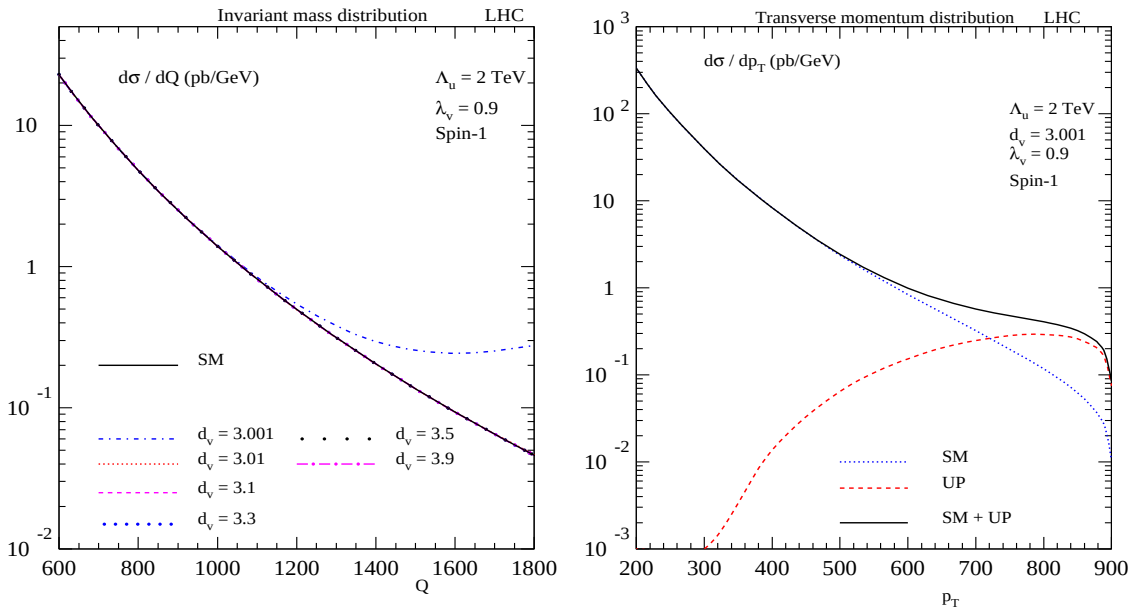


Figure 5: Invariant di-jet mass distribution and $p_T$ distribution for spin-1 unparticles for $\Lambda_u$ =2TeV. Left Panel: Variation of the signal with scaling dimension $d_v$. Right panel: $p_T$ distribution for $d_v = 3.001$

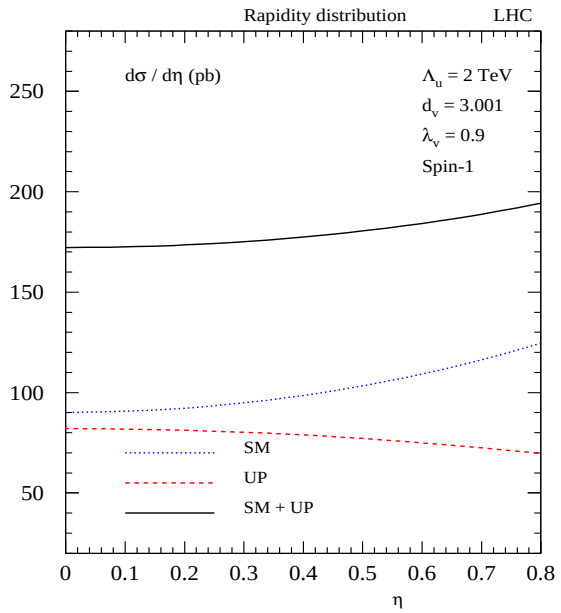


Figure 6: Rapidity distribution for spin-1 unparticles for $\Lambda_u$ =2TeV and $d_v = 3.001$

| subprocess | $\overline{\sum}\|M\|^2$ |
|---|---|
| $qq' \to qq'$ | $\frac{f_N}{2}\ \frac{s^2+u^2}{t^2}$ |
| $qq \to qq$ | $\frac{f_N}{2}\ \left(\frac{u^2+s^2}{t^2}+\frac{t^2+s^2}{u^2}\right)-\frac{f_N}{N}\ \frac{s^2}{ut}$ |
| $q\overline{q} \to q\overline{q}$ | $\frac{f_N}{2}\ \left(\frac{u^2+t^2}{s^2}+\frac{u^2+s^2}{t^2}\right)-\frac{f_N}{N}\ \frac{u^2}{st}$ |
| $q\overline{q} \to q'\overline{q}'$ | $\frac{f_N}{2}\ \frac{u^2+t^2}{s^2}$ |
| $q\overline{q} \to gg$ | $\frac{Nf_N}{2}\ \frac{(u^2+t^2)^2}{uts^2}-\frac{f_N}{2N}\ \frac{u^2+t^2}{ut}$ |
| $gg \to q\overline{q}$ | $\frac{1}{2N}\ \frac{(u^2+t^2)^2}{uts^2}-\frac{1}{N^3 f_N}\ \frac{u^2+t^2}{s^2}$ |
| $qg \to qg$ | $\frac{(u^2+s^2)}{t^2}-\frac{f_N}{2}\ \frac{u^2+s^2}{us}$ |
| $gg \to gg$ | $\frac{4}{f_N}\ \frac{\left(s^2+su+u^2\right)^3}{s^2u^2t^2}$ |

Table 1: Matrix elements for the Standard Model. $s=(p_1+p_2)^2, t=(p_1-p_3)^2, u=(p_1-p_4)^2$ and $f_N=(N^2-1)/N^2$

| subprocess | $\overline{\sum}\lvert\mathcal{M}_u\rvert^2$ | $2\ \mathcal{R}e\Big(\mathcal{M}_u\mathcal{M}^*_{SM}\Big)$ |
|---|---|---|
| $qq\prime \to qq\prime$ | $\mathcal{D}_t^2\ t^2$ | $0$ |
| $qq \to qq$ | $\frac{1}{N}\mathcal{D}_t\mathcal{D}_u\ tu + \mathcal{D}_t^2\ t^2 + \mathcal{D}_u^2\ u^2$ | $f_N\ \Big(\mathcal{D}_u\ \frac{u^2}{t} + \mathcal{D}_t\ \frac{t^2}{u}\Big)$ |
| $q\overline{q} \to q\overline{q}$ | $\frac{1}{N}\ \mathcal{D}_t Re(\mathcal{D}_s)\ st + \mathcal{D}_t^2\ t^2 + \lvert\mathcal{D}_s\rvert^2\ s^2$ | $f_N\ \Big(Re(\mathcal{D}_s)\ \frac{s^2}{t} + \mathcal{D}_t\ \frac{t^2}{s}\Big)$ |
| $q\overline{q} \to q\prime\overline{q}\prime$ | $\lvert\mathcal{D}_s\rvert^2\ s^2$ | $0$ |

Table 2: Matrix elements for scalar unparticle in fermion initiated processes $f_N = (N^2 - 1)/N^2$

| subprocess | $\overline{\sum}\lvert\mathcal{M}_u\rvert^2$ | $2\ \mathcal{R}e\Big(\mathcal{M}_u\mathcal{M}^*_{SM}\Big)$ |
|---|---|---|
| $qq\prime \to qq\prime$ | $2\mathcal{D}_t^2\ \left(2u^2 + 2ut + t^2\right)$ | $0$ |
| $qq \to qq$ | $2\Big(\frac{2}{N}\mathcal{D}_t\mathcal{D}_u\ \left(u^2 + 2ut + t^2\right) + \mathcal{D}_t^2\ \left(2u^2 + 2tu + t^2\right)$ $+\mathcal{D}_u^2\ \left(u^2 + 2tu + 2t^2\right)\Big)$ | $-2g_s^2 f_N\ s^2\ \Big(\frac{\mathcal{D}_u}{t} + \frac{\mathcal{D}_t}{u}\Big)$ |
| $q\overline{q} \to q\overline{q}$ | $2\Big(\frac{2}{N}\ \mathcal{D}_t Re(\mathcal{D}_s)\ u^2 + \mathcal{D}_t^2\ \left(2u^2 + 2tu + t^2\right)$ $+\lvert\mathcal{D}_s\rvert^2\ \left(u^2 + t^2\right)\ Big)$ | $-2g_s^2 f_N\ u^2\ \Big(\frac{Re(\mathcal{D}_s)}{t} + \frac{\mathcal{D}_t}{s}\Big)$ |
| $q\overline{q} \to q\prime\overline{q}\prime$ | $2\lvert\mathcal{D}_s\rvert^2\ \left(u^2 + t^2\right)$ | $0$ |

Table 3: Matrix elements for spin-1 unparticle in fermion initiated processes $f_N = (N^2 - 1)/N^2$

| subprocess | $\overline{\sum}\lvert\mathcal{M}_u\rvert^2$ | $2\ \mathcal{R}e\Big(\mathcal{M}_u\mathcal{M}_{SM}^*\Big)$ |
|---|---|---|
| $qq\prime \to qq\prime$ | $\frac{1}{128}\mathcal{D}_t^2\ \Big(u^4+s^4\ -6su\big[u^2+s^2-3su\big]\Big)$ | $0$ |
| $qq \to qq$ | $\frac{1}{128N}\Big(N\mathcal{D}_t^2\big[u^4+s^4-6su\ \big(u^2+s^2-3su\big)\big]$ $+\mathcal{D}_t\mathcal{D}_u s^2\big[4s^2+9ut\big]\Big)+t\leftrightarrow u$ | $-\frac{1}{8}\mathcal{D}_u f_N\ (3u+4s)\frac{s^2}{t}-(u\leftrightarrow t)$ |
| $q\overline{q} \to q\overline{q}$ | $\frac{1}{128N}\Big(ND_t^2\big[u^4+s^4-6su\ \big(u^2+s^2-3su\big)\big]$ $+\mathcal{R}e\left(\mathcal{D}_t\mathcal{D}_s\right)u^2\big[9ts+4u^2\big]\Big)+t\leftrightarrow s$ | $-\frac{1}{8}f_N\Big(\mathcal{R}e(\mathcal{D}_s)\ (3s+4u)\frac{u^2}{t}$ $-\mathcal{D}_t\ (3t+4u)\frac{u^2}{s}\Big)$ |
| $q\overline{q} \to q\prime\overline{q}\prime$ | $\frac{1}{128}\lvert\mathcal{D}_s\rvert^2\ \Big(u^4+t^4\ -6tu\ \big[u^2+t^2-3tu\big]\ \Big)$ | $0$ |
| $q\overline{q} \to gg$ | $\frac{1}{8}Nf_N\lvert\mathcal{D}_s\rvert^2\ ut\Big(u^2+t^2\Big)$ | $-\frac{1}{2}f_N\mathcal{R}e(\mathcal{D}_s)\ \Big(u^2+t^2\Big)$ |
| $gg \to q\overline{q}$ | $\frac{1}{8}\frac{1}{Nf_N}\lvert\mathcal{D}_s\rvert^2\ ut\Big(u^2+t^2\Big)$ | $-\frac{1}{2(N^2-1)}\mathcal{R}e(\mathcal{D}_s)\ \Big(u^2+t^2\Big)$ |
| $qg \to qg$ | $-\frac{1}{8}\mathcal{D}_t^2\ us\Big(u^2+s^2\Big)$ | $\frac{1}{2N}\mathcal{D}_t\ \Big(u^2+s^2\Big)$ |
| $gg \to gg$ | $\frac{2}{8(N^2-1)}\ \Big(\mathcal{D}_u\mathcal{R}e(\mathcal{D}_s)\ t^4+\mathcal{D}_t\mathcal{R}e(\mathcal{D}_s)\ u^4$ $+\mathcal{D}_t\mathcal{D}_u\ s^4\Big)+\frac{1}{8}\mathcal{D}_u^2\ \left(t^4+s^4\right)$ $+\frac{1}{8}\mathcal{D}_t^2\ \left(u^4+s^4\right)+\frac{1}{8}\lvert\mathcal{D}_s\rvert^2\ \left(t^4+u^4\right)$ | $-\frac{1}{Nf_N}\Big(\mathcal{D}_u\frac{t^4+s^4}{st}+\mathcal{D}_t\frac{u^4+s^4}{su}$ $+\mathcal{R}e(\mathcal{D}_s)\frac{t^4+u^4}{ut}\Big)$ |

Table 4: Matrix elements for spin 2 unparticle